

**Registry No.** Polyethylene (homopolymer), 9002-88-4; polypropylene (homopolymer), 9003-07-0.

## References and Notes

- (1) P. J. Flory, "Statistical Mechanics of Chain Molecules", Interscience, New York, 1968.
- (2) J. Rault, M. Sotton, C. Rabourdin, and E. Robelin, *J. Phys. (Paris)*, **41**, 1459, 1469 (1980).
- (3) J. Rault and E. Robelin, *Polym. Bull.*, **2**, 373 (1980); J. Rault, *J. Am. Phys. Soc.*, **27**, 258 (1982).
- (4) E. Robelin-Souffaché and J. Rault, *Macromolecules*, preceding paper in this issue.
- (5) W. W. Graessley and S. F. Edwards, *Polymer*, **22**, 1329 (1981).
- (6) V. R. Raju, G. Smith, G. Marin, J. R. Know, and W. W. Graessley, *J. Polym. Sci.*, **17**, 1183 (1975).
- (7) W. W. Graessley, *Adv. Polym. Sci.*, **16**, 1 (1974).
- (8) P.-G. de Gennes, "Scaling Concepts in Polymers Physics", Cornell University Press, Ithaca, NY, 1979.
- (9) J. Klein, *Nature (London)*, **271**, 143 (1978); *Macromolecules*, **11**, 852 (1978).
- (10) D. C. Prevorsek and B. T. de Bona, *J. Macromol. Sci., Phys.*, **B19**, 605 (1981).
- (11) G. P. Andrianova, *J. Polym. Sci., Phys.*, **13**, 95 (1975).
- (12) L. Wild, R. Ranganath, and D. C. Knobloch, *Polym. Eng. Sci.*, **16**, 12, 811 (1976).

# Viscoelastic Properties of Blends of Styrene-Butadiene Diblock Copolymer and High Molecular Weight Homopolybutadiene

Hiroshi Watanabe and Tadao Kotaka\*

Department of Macromolecular Science, Faculty of Science, Osaka University, Toyonaka, Osaka 560, Japan. Received April 15, 1983

**ABSTRACT:** Viscoelastic properties of three well-characterized styrene-butadiene (SB) diblock copolymers blended with three high molecular weight homopolybutadienes (hB) were examined. Since hB is a nonsolvent for S blocks, micelles with precipitated S cores and dissolved B cilia are formed in the blends. The blend exhibits a shoulder or plateau often called a second plateau in the low-frequency region of the storage  $G'$  and loss  $G''$  moduli. When the SB content  $c$  is smaller than a certain critical value  $c_b^*$ , the frequency region where the second plateau appears is independent of  $c$ . On the other hand, when  $c$  is increased beyond  $c_b^*$ , the second plateau rapidly extends to the lower frequency region. This critical value  $c_b^*$  coincides with the concentration at which the micelles begin to contact and their cilia begin to overlap with each other. These results suggest that the slow relaxation mechanism for the blends with  $c$  below  $c_b^*$  may be related to the motion of the B cilia entangled with the matrix hB molecules, while that for the blends with  $c$  above  $c_b^*$  is related to the delayed reptation of the mutually entangled B cilia of the neighboring micelles. From this viewpoint, we are able to explain the dependence of the longest relaxation time  $\tau_p$  of the blends on the SB content  $c$  and on the molecular weights  $M_{bB}$  and  $M_{hB}$  of the B block and hB molecules, respectively, by employing the "tube renewal" mechanism of Klein and the modified "tube" model of Doi and Edwards and of Kuzuu for star polymers.

## I. Introduction

In our previous papers,<sup>1-3</sup> we described rheological properties of blends of styrene-butadiene (SB) diblock copolymers (with S content less than 30 wt %) and a low molecular weight homopolybutadiene (with an  $M_n$  of about  $2 \times 10^3$ , coded as chB). The behavior of the blends was basically linear viscoelastic but was quite different from that of ordinary homopolymers in concentrated solutions and melts.<sup>4,5</sup> Namely, as the SB content  $c$  is increased beyond a certain critical value  $c_b^*$ , the blends begin to exhibit a slow relaxation process in the low-frequency region,<sup>1-3</sup> where an ordinary homopolymer system has no such processes but exhibits a Newtonian flow.<sup>4,5</sup>

We proposed the following mechanism for such a slow relaxation process found in the SB/chB blends.<sup>3</sup> Since chB itself is a  $\theta$  solvent for B blocks but a nonsolvent for S blocks, SB molecules tend to aggregate and form micelles with precipitated S cores and dissolved B cilia. With increasing SB content  $c$ , the B cilia of neighboring micelles begin to overlap and entangle with one another. The slow relaxation process is a result of retarded reptational motion of the mutually entangled B cilia, because the reptational motion of a polymer chain (in this system, a B cilium) with one end fixed and the other end free would be highly retarded as pointed out by de Gennes.<sup>6</sup>

However, in this earlier study<sup>3</sup> we did not observe the entanglement effect of chB molecules on the relaxation processes, presumably because the  $M_n$  of chB was too small to result in effective entanglements. In other words, only the entanglement network resulting from B cilia alone

Table I  
Characteristics of Polymer Samples

code	$10^{-3}M_n$	$M_w/M_n$	wt % of PS	$10^{-3}M_n$ of S block	$10^{-3}M_n$ of B block
SB3	134	1.07	24.0	32	102
SB4	192	1.08	17.0	32	160
SB5	294	1.10	11.0	32	262
hB1	27.6	1.05	0	0	27.6
hB2	60.7	1.05	0	0	60.7
hB3	177	1.06	0	0	177

affected the slow relaxation process in the SB/chB blends. To clarify the effect of entanglements between matrix homopolybutadiene and B cilia of the micelles, we examined viscoelastic properties of blends of SB diblock copolymers and high molecular weight homopolybutadiene with  $M_n$  at least a few times greater than the average molecular weight  $M_e^{\text{bulk}}$  between entanglement points in bulk homopolybutadiene.<sup>4,5</sup> The mechanisms of slow relaxation processes in such blends will be discussed in terms of the tube model<sup>7-10</sup> for B cilia entangled with matrix homopolybutadiene and with B cilia of neighboring micelles.

## II. Experimental Section

**1. Materials.** Three SB diblock copolymers, SB3, SB4, and SB5, employed in this study were prepared by anionic polymerization using *sec*-butyllithium as the initiator and benzene as the solvent.<sup>11</sup> All of these SB samples were prepared from the same batch of precursor living polystyrene (PS) and, therefore, have S blocks of the same characteristics. Three homopoly-

butadiene samples, hB1, hB2, and hB3, were also synthesized by anionic polymerization using the same initiator and solvent as the SB samples. Table I shows the characteristics of these SB and hB samples determined by a gel permeation chromatograph equipped with a triple-detector system consisting of a refractometer, an UV-absorption monitor, and a low-angle laser-light scattering photometer (Toyo Soda Ltd., System HLC 801A-UV8-LS8).<sup>11</sup> It has been known that hB is miscible with B blocks of SB molecules only when the molecular weight  $M_{hB}$  of the hB is lower than that of the B blocks  $M_{bB}$ .<sup>12,13</sup> On the other hand, when the molecular weights  $M_{bS}$  and  $M_{hB}$  of the blocks are too small, the microphase separation between the S and B blocks does not take place.<sup>14</sup> We prepared six blends: SB3/hB1, SB4/hB1 and -hB2, and SB5/hB1, -hB2, and -hB3. These blends satisfy the above two criterions. In fact, we confirmed the presence of spherical S microdomains randomly dispersed in the B matrix phase in SB/chB blends, which are similar to the blends examined here.<sup>1,15</sup>

To prepare a blend, we dissolved prescribed amounts of the SB, hB, and an antioxidant, butylhydroxytoluene (BHT; about 1 wt % of the blend), in a large amount of methylene chloride, which was subsequently evaporated to obtain a blend of desired composition.

**2. Rheological Measurements.** Dynamic measurements were made with a conventional rheometer (an Autoviscometer L-III, Iwamoto Seisakusho, Kyoto) equipped with a cone-and-plate assembly. The radius of the cone was 15.0 mm, and the angle between the cone and plate was 3.68°. The measurements were carried out at several temperatures below 160 °C. To suppress cross-linking and oxidative degradation of B segments, we carried out the measurements at temperatures between 50 and 160 °C under a stream of nitrogen. To eliminate the prehistory of the microphase-separated structure during the blend preparation, the blends were annealed at about 80 °C for 20 min before measurements were made. In this way, we could obtain a reproducible (and presumably close to an equilibrium) domain structure.<sup>15</sup> The angular frequency  $\omega$ /(rad s<sup>-1</sup>) was examined between 0.01 and 5. Under these conditions all the blends exhibited linear viscoelastic behavior as long as the amplitude of strain was kept below 0.3. Especially at the highest temperature examined, they exhibited almost Newtonian behavior. The data were analyzed by using the Markovitz equation<sup>16</sup> to determine the storage  $G'$  and loss  $G''$  moduli. The time-temperature superposition principle<sup>6</sup> was applied to obtain the master curves. In general, multiphase systems such as the block copolymer systems do not obey the time-temperature superposition principle. However, the superposition worked well for the present blends, presumably because of the low total styrene content (<3 wt %) and also because of the large difference in the glass transition temperatures of the S and B blocks.

### III. Results and Discussion

**1. Master Curves and Relaxation Spectra.** Figure 1 shows the master curves of the storage  $G'$  and loss  $G''$  moduli for the SB5/hB1 blends reduced to 27 °C. The numbers attached to the curves represent the SB5 content  $c$  in wt %. As seen in the figures, a shoulder appears in both the  $G'$  and  $G''$  curves for the blend with  $c$  as small as 1 wt %. The frequency region where the shoulder appears is independent of  $c$  as long as  $c$  is below a certain critical value  $c_b^*$  (4 wt % for the SB5/hB1 blend). A similar shoulder was not observed in any SB/chB blends.<sup>3</sup> As  $c$  increases beyond the critical value  $c_b^*$ , the shoulder develops into a plateau and the plateau region becomes extended rapidly toward the low-frequency side, as was observed for SB/chB blends.<sup>3</sup> Although the figures are not shown here, essentially the same behavior was observed for other blends examined in this study.

Figure 2 shows the temperature dependence of the shift factor  $a_T$  for all the SB/hB blends, including hB samples. The solid curve in the figure represents the WLF relation<sup>5</sup> with  $C_1 = 8.86$  and  $C_2 = 101.6$ , and the reference temperature  $T_s$  of -60 °C. This value of  $T_s$  chosen for the blends is the same as that determined for anionically po-

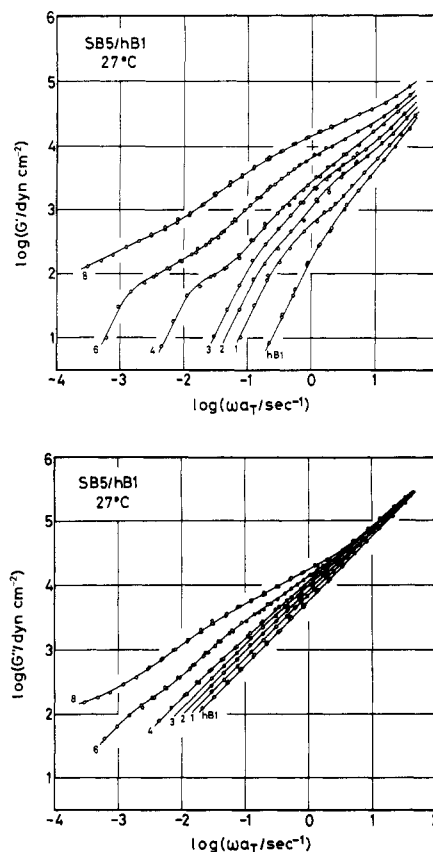


Figure 1. Master curves of the storage  $G'$  and loss  $G''$  moduli of the SB5/hB1 blends reduced to 27 °C. The numerical values in the figure represent the content of SB5 in wt %.

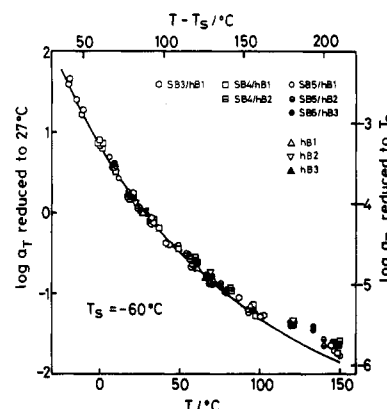


Figure 2. Temperature dependence of the shift factor  $a_T$  for the SB/hB blends and hB samples. The solid curve in the figure represents the WLF relation with the reference temperature  $T_s = -60$  °C.

lymerized homopolybutadiene.<sup>6</sup> At temperatures above  $T_g + 150$  °C, the data points deviate slightly from the WLF curve. However, even at these high temperatures the log  $a_T$  shows the same temperature dependence for all the blends including hB samples. In fact, this result was also obtained for all the SB/chB blends, which showed an Arrhenius-type dependence of log  $a_T$  on temperature.<sup>3</sup>

Figure 3 shows the relaxation spectra  $H(\log \tau)$  calculated from the master curves of  $G'$  and  $G''$  by using the Tschoegl approximation.<sup>17</sup> The numbers in the figure represent the SB content  $c$  in wt %. The spectra calculated from the  $G'$  and  $G''$  curves for the same blend coincide with each other within the error of approximation. For the spectra, we notice that the position of the shoulder or peak does not depend on  $c$  for the blends with  $c$  below  $c_b^*$ . On the other hand, the peak position rapidly shifts to a longer time

Table II  
Comparison of the Observed and Estimated Critical SB  
Content of the SB/hB Blends

sample	obsd $c_b^*/\text{wt } \%$	estimated	
		$c_1^*/\text{wt } \%$	$c_2^*/\text{wt } \%$
SB3/hB1	5-6	3.9	7.4
SB3/chB <sup>a</sup>			
SB4/hB1			
SB4/hB2	4-5	3.8	7.3
SB4/chB <sup>a</sup>			
SB5/hB1			
SB5/hB2	3-4	3.1	6.0
SB5/hB3			
SB5/chB <sup>a</sup>			

<sup>a</sup> See ref 3.

side with increasing  $c$  above  $c_b^*$ . In Table II, we compare the values of  $c_b^*$  for the SB/hB blends examined in this study with those of SB/chB blends examined in the previous study.<sup>3</sup> The observed  $c_b^*$  is independent of the molecular weight  $M_{hB}$  of the matrix hB molecules but is dependent on the molecular weight  $M_{SB}$  (and the S content) of the SB copolymer involved.

As in the previous study,<sup>3</sup> we calculate two critical concentrations  $c_1^*$  and  $c_2^*$  as follows.

$$c_i^*/(\text{wt } \%) = \frac{100f_i}{\rho} \frac{N_m M_{SB}}{(R_B + r_s)^3 N_A} \quad i = 1 \text{ or } 2 \quad (1)$$

Here,  $N_m$  is the number of SB molecules forming one micelle,  $M_{SB}$  the molecular weight of the SB molecule,  $R_B$  the thickness of the ciliary B layer,  $r_s$  the radius of the S core,  $\rho$  the density of the blend, and  $N_A$  the Avogadro number (cf. Figure 6). The numerical factor  $f_i$  is given as  $f_1 = 1/8$  and  $f_2 = 3/4\pi$ . For  $N_m$  and  $r_s$ , we employed the values already determined for the same SB's in *n*-tetradecane solutions by a small-angle X-ray scattering (SAXS) study,<sup>11</sup> as was done for SB/chB blends in the previous study.<sup>3</sup> The  $R_B$  was calculated as the unperturbed root-mean-square end-to-end distance of the B block as  $R_B = b n_{hB}^{1/2}$ , with  $b$  and  $n_{hB}$  being the step length and the number of B segments in a B block, respectively. In short,  $c_1^*$  is the average concentration at which the micelles at the surface of the B layer begin to touch each other, while  $c_2^*$  is that at which the segments of the B blocks begin to occupy the matrix phase uniformly, i.e., the critical threshold.<sup>6</sup> The values of  $c_1^*$  and  $c_2^*$  are also listed in Table II. We notice that  $c_b^*$  falls between  $c_1^*$  and  $c_2^*$ , close to  $c_1^*$ .

We estimated the longest relaxation time  $\tau_p$  at 27 °C from the inflection point of the shoulder or the peak

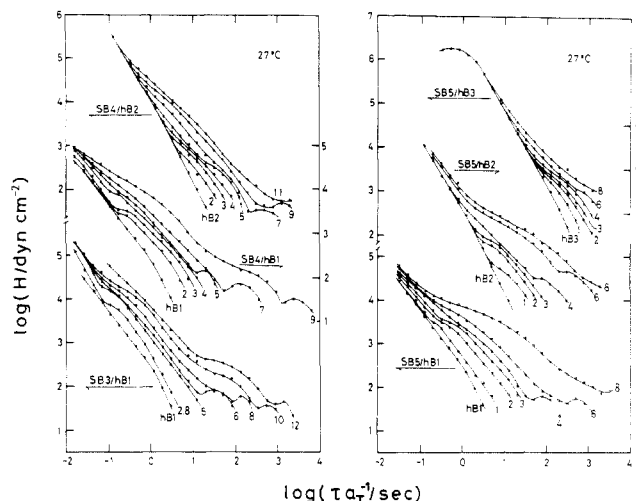


Figure 3. Relaxation spectra for the SB/hB blends and hB samples reduced to 27 °C calculated from the master curves of the dynamic moduli.

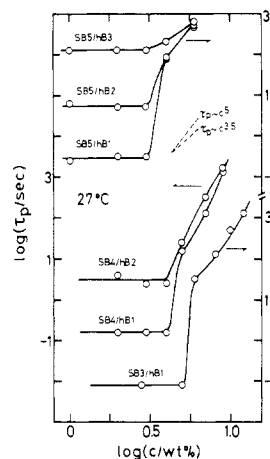
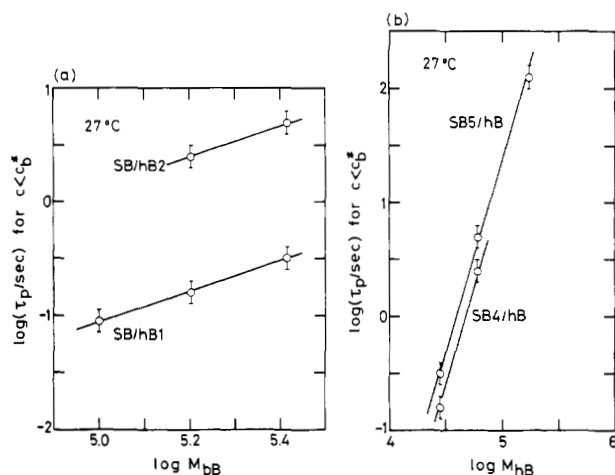


Figure 4. SB content dependence of the longest relaxation time  $\tau_p$  of the SB/hB blends reduced to 27 °C. The broken lines in the figure represent the power-law-type dependences as indicated.

position of the relaxation spectra of the SB/hB blends. Figure 4 shows the plots of  $\tau_p$  against the SB content  $c$ . The values of  $\tau_p$  are also tabulated in Table III. In the region of  $c$  below  $c_b^*$ ,  $\tau_p$  is dependent on the molecular weight of the B block  $M_{hB}$  as well as  $M_{SB}$  but is independent of  $c$ . On the other hand, in the region of  $c$  above  $c_b^*$ ,  $\tau_p$  is strongly dependent on  $c$  as well as on  $M_{hB}$  but becomes independent of  $M_{hB}$ . The features of  $\tau_p$  for the blends with  $c$  well above  $c_b^*$  are essentially the same as

Table III  
Longest Relaxation Time  $\tau_p$  of the SB/hB Blends at 27 °C

SB3/hB1								
SB3 content/wt %	2.8	5	$c_b^*$	6	8	10	12	
$\log \tau_p/s$								
SB3/hB1	-1.1	-1.1		1.5	2.1	2.7	3.1	
SB4/hB1 and -hB2								
SB4 content/wt %	2	3	4	$c_b^*$	5	7	9	11
$\log \tau_p/s$								
SB4/hB1	-0.8	-0.8	-0.8		1.2	2.1	3.2	
SB4/hB2	0.6	0.4	0.4		1.4	2.5	3.1	>3.5
SB5/hB1, -hB2, and -hB3								
SB5 content/wt %	1	2	3	$c_b^*$	4	6	8	
$\log \tau_p/s$								
SB5/hB1	-0.6	-0.5	-0.5		1.9	2.7	>3.5	
SB5/hB2	0.8	0.7	0.7		1.9	2.6	>3.3	
SB5/hB3	2.1	2.1	2.1		2.3	2.8	>3.0	



**Figure 5.** Dependence of the longest relaxation time  $\tau_p$  of the SB/hB blends having SB content smaller than the critical value on (a) the molecular weight  $M_{bB}$  of the B block and (b) on the molecular weight  $M_{hB}$  of the hB molecules reduced to 27 °C. The solid lines in the figure represent the relations (a)  $\tau_p \propto M_{bB}^{1.46}$  and (b)  $\tau_p \propto M_{hB}^{3.4}$ .

those for the SB/chB blends in the same region.<sup>3</sup> Parts a and b of Figure 5 show double-logarithmic plots of  $\tau_p$  and  $M_{bB}$  and of  $\tau_p$  and  $M_{hB}$ , respectively, in the region of  $c$  below  $c_b^*$ . These results may be cast in a form

$$\tau_p/s = (3.2 \times 10^{-24}) M_{bB}^{1.46} M_{hB}^{3.4} \quad (27^\circ\text{C}) \quad (2)$$

**2. Molecular Mechanisms of the Slow Relaxation Process.** The results mentioned in the preceding section suggest that there are two mechanisms in the slow relaxation process of the SB/hB blends. The first is for blends with  $c$  below  $c_b^*$ , and the other for blends with  $c$  above  $c_b^*$ .

Figure 6 illustrates the possible schemes of the slow relaxation processes in terms of a tube model<sup>7-10</sup> and a tube renewal (or reorganization) process.<sup>18-21</sup> For a blend with  $c$  below  $c_b^*$ , the B cilia of the neighboring micelles do not overlap (Figure 6a). In this case, only hB molecules entangle with the B cilia and form a tube for each B cilium (Figure 6b). The entangled B cilium (bB chain) would relax either by a reptation of the cilium itself or by a tube renewal due to the reptation of the hB molecules forming the tube.

For a monodisperse and long linear chain system, the time scale for the reptation of a chain to escape from a tube surrounding it should be much shorter than that for the renewal of the tube,<sup>18-21</sup> because the tube renewal process requires the reptation of many chains (equivalent to the given chain) forming the tube. Thus, in such a system, the polymer chain escapes from the tube by reptation of itself and relaxes. However, for the present SB/hB blends the time scale for the reptation of the B cilium would be much longer than that for the renewal of the tube composed of hB molecules, because one end of each B cilium is fixed on a rigid S core so that its reptation is highly retarded<sup>6</sup> and also because  $M_{bB}$  is larger than  $M_{hB}$ . Thus, for the SB/hB blends with  $c$  below  $c_b^*$  the renewal of the hB tube prevails over the retarded reptation of the B cilium, and the B cilium relaxes mainly by the tube renewal process (Figure 6b). The relaxation time  $\tau_p$  for this process is obviously independent of  $c$ .

When  $c$  exceeds  $c_b^*$ , the B cilia of the neighboring micelles overlap each other (Figure 6c). In such a case, both hB molecules and B blocks of the neighboring micelles form a tube for a B cilium (Figure 6d). When the extent of overlapping is not very large, i.e., the  $c$  is not much larger than  $c_b^*$ , the B blocks belonging to neighboring micelles form a tube only near the free end of the particular B

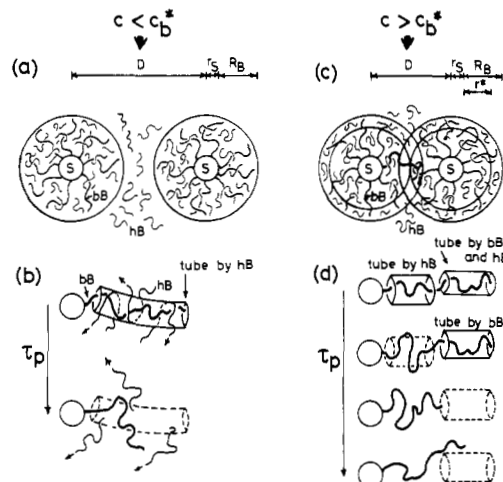


**Figure 6.** Schematic diagram explaining the slow relaxation mechanisms of the SB/hB blends having SB content  $c$  below and above the critical value  $c_b^*$ . The symbols  $D$ ,  $r_s$ , and  $R_B$  represent the mean distance between the centers of the neighboring micelles, the radius of the S core, and the thickness of the B block layer, respectively. For details, see text.

cilium. This B cilium (bB) would relax either by the reptation of bB itself or by the tube renewal. With further increasing  $c$  beyond  $c_b^*$ , the extent of mutual entanglements between the B cilia of the neighboring micelles becomes greater (Figure 6d). The time required for renewal of the part of the tube composed of hB molecules will remain nearly the same as that for the blends with  $c$  below  $c_b^*$ . However, the part of the tube composed of B blocks will persist for a considerably longer time (Figure 6d), because the renewal of this bB tube requires the reptation of many B cilia. Thus, for the blends with  $c$  well above  $c_b^*$ , an entrapped B cilium would relax only by its reptation, as was the case for the concentrated SB/chB blends.<sup>3</sup> As discussed in the previous paper,<sup>3</sup> this type of slow relaxation process may be explained by extending the Doi-Kuzuu theory<sup>10</sup> of the tube model for star-shaped homopolymers. The reptation of the B cilium becomes difficult when the extent of micelle overlapping becomes larger and the tube composed of B blocks becomes longer.<sup>3</sup> Therefore, the time required for the reptation of the B cilium increases rapidly with SB content. For the blends with  $c$  below and above  $c_b^*$ , the time  $\tau_p$  for the processes described above are theoretically estimated and compared with the experimental data as follows.

**$\tau_p$  in the Region of  $c$  below  $c_b^*$ .** Doi,<sup>18</sup> de Gennes,<sup>19</sup> Klein,<sup>20</sup> and Graessley<sup>21</sup> calculated the time required for the tube renewal in monodisperse homopolymer systems. According to Klein,<sup>20</sup> the tube itself is regarded as a (virtual) Rouse chain consisting of  $N_{\text{sub}}$  (virtual) submolecules, whose size is assumed to be the distance between the adjacent entanglement points along the chain. The time  $\tau_p$  required for the tube renewal process is estimated as the longest relaxation time of the virtual Rouse chain (tube) as<sup>20</sup>

$$\tau_p \approx N_{\text{sub}}^2 \tau_{\text{rep}} / 18\pi^2 \quad (3)$$

where  $\tau_{\text{rep}}$  is the reptational time of the (actual) polymer chain forming the tube.

For the SB/hB blends with  $c$  below  $c_b^*$ , the length of the tube composed of the hB molecules is assumed to be proportional to the length of the B cilium entrapped in this tube. Thus, eq 3 is rewritten for our blends as

$$\tau_p \approx (n_{bB}/n_e^{\text{bulk}})^2 \tau_{\text{rep}}^{\text{hB}} / 18\pi^2 \quad (3')$$

where  $n_{bB}$  ( $=M_{bB}/54$ ) is the degree of polymerization of

the B block,  $\tau_{\text{rep}}^{\text{hB}}$  the reptational time of hB, and  $n_e^{\text{bulk}}$  the number of the segments between the adjacent entanglement points in bulk polybutadiene. For anionically polymerized homopolybutadiene by the method employed in the present study, the value of  $n_e^{\text{bulk}} = 37$  is reported.<sup>4,5</sup> For  $\tau_{\text{rep}}^{\text{hB}}$ , we assume the following equation

$$\tau_{\text{rep}}^{\text{hB}}/\text{s} = (7.2 \times 10^{-19})M_{\text{hB}}^{3.4} \quad (27^\circ\text{C}) \quad (4)$$

because the molecular weight of the hB samples examined in this study is sufficiently higher than that between the entanglement points ( $\approx 2000$ ).<sup>4,5</sup> The numerical prefactor in eq 4 is determined from the longest relaxation time for the hB3 sample ( $\approx 0.5$  s, estimated from the peak position of the relaxation spectrum shown in Figure 3 and its molecular weight). Employing eq 4, we rewrite eq 3' as

$$\tau_p/\text{s} \approx (1.0 \times 10^{-27})M_{\text{hB}}^2 M_{\text{hB}}^{3.4} \quad (27^\circ\text{C}) \quad (3'')$$

By comparing eq 2 and 3'', we notice the following points. The dependence of  $\tau_p$  on  $M_{\text{hB}}$  of eq 2 coincides with that of eq 3''. Even when the tube is regarded as a virtual chain other than the Rouse chain, the dependence of  $\tau_p$  on  $M_{\text{hB}}$  and  $M_{\text{hB}}$  should be separated and the  $M_{\text{hB}}$  dependence should be given as  $M_{\text{hB}}^{3.4}$ . The  $\tau_{\text{rep}}^{\text{hB}} (\propto M_{\text{hB}}^{3.4})$  determines the mobility of a submolecule in a virtual chain, and  $M_{\text{hB}}$  determines the length of the virtual chain. On the other hand, the dependence of  $\tau_p$  on  $M_{\text{hB}}$  of eq 2 is weaker than that of eq 3''. The observed  $M_{\text{hB}}$  dependence ( $\tau_p \propto M_{\text{hB}}^{1.46}$ ) is close to that of the Zimm chain rather than that of the Rouse chain employed by Klein. The exponent for  $M_{\text{hB}}$  is dependent on the type of virtual chain employed. Klein<sup>20</sup> employed the free-draining approximation at all distances and assumed that the distance between the entanglement points is sufficiently larger than the monomer size. These assumptions are not necessarily valid. The substitution of  $N_{\text{sub}}$  by  $n_{\text{bB}}/n_e^{\text{bulk}}$  made in eq 3' is also not necessarily correct, because the segments of the B block near the free end may move more freely than those near the anchored end. Namely, the tube renewal process for a free linear chain is not necessarily the same as that for a B cilium with a fixed end. Although the difficulty described above still remains, the comparison of eq 3'' (theory) and eq 2 (experiment) suggests that the slow relaxation process for the blends with  $c$  below  $c_b^*$  is attributable to the tube renewal process such as shown schematically in Figure 6b. However, we should note that the prefactor in eq 2 is about  $10^3$  times larger than that in eq 3''. Graessley's result is similar to eq 3, but his numerical factor is about  $1/\pi^2$  instead of  $1/18\pi^2$  as given by Klein. If we employ the Graessley equation, the difference between eq 2 and 3'' becomes smaller, but a considerable discrepancy (of the order  $10^2$ ) still remains. This discrepancy is discussed later.

**$\tau_p$  in the Region of  $c$  above  $c_b^*$ .** For the blends with  $c$  above  $c_b^*$ , the  $\tau_p$  becomes independent of  $M_{\text{hB}}$  when  $c$  is further increased beyond  $c_b^*$  (see Figure 4). This result indicates that the time for renewal of the part of the tube composed of hB molecules is much shorter than the longest relaxation time  $\tau_p$  of the blend. Thus, for the estimation of  $\tau_p$  in this region, the hB molecules may be regarded as a uniform medium which does not contribute to the entanglements lasting for a long time. It would be sufficient to consider only the tube formed near the free end of the B cilium by the B blocks of neighboring micelles (Figure 6d). Then, the previously proposed version<sup>3</sup> of the Doi-Kuzuu theory<sup>10</sup> on the reptation of a polymer chain with a fixed end would be valid for the blend with  $c$  above  $c_b^*$ . When the B cilium escapes from the tube by its reptation, the end-to-end distance of the cilium must become shorter

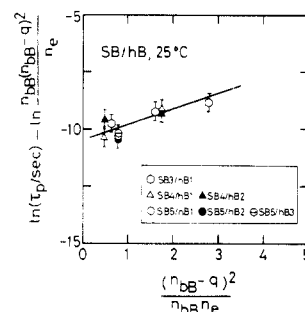


**Figure 7.** Plots of  $\ln \tau_p - \ln [n_{\text{bB}}(n_{\text{bB}} - q)^2 / n_e]$  vs.  $(n_{\text{bB}} - q)^2 / (n_{\text{bB}} n_e)$  of the SB/hB blends reduced to  $25^\circ\text{C}$ . The symbol  $\ln$  represents the natural logarithm. The parameters  $q$ ,  $n_e$ ,  $n_{\text{bB}}$ , and  $\tau_p$  are the number of the untrapped segments per B block, the number of segments between the adjacent entanglement points in the blend, the degree of polymerization of the B block, and the longest relaxation time of the blend, respectively.

than that at the equilibrium because the anchored end cannot move (Figure 6d), and extra (free) energy  $\Delta U$  is required for this process. Doi and Kuzuu regarded this process as an activation process, and defined the time  $\tau_p$  required for this process as<sup>10</sup>

$$\tau_p \approx \tau^{(1)} \exp(\Delta U/kT) \quad (5)$$

where  $\tau^{(1)}$  is the time required for a free chain with no fixed ends to escape from the tube by reptation.

For the SB/hB blends,  $\tau^{(1)}$  and  $\Delta U$  are written in terms of the number  $q$  of the B cilium segments that are not trapped in the tube and the number  $n_e$  of the segments between the adjacent entanglement points in the tube (entanglement) region.<sup>3</sup> Then, eq 5 is rewritten as<sup>3</sup>

$$\tau_p \approx \frac{\zeta \nu^2 b^2}{kT} \frac{n_{\text{bB}}(n_{\text{bB}} - q)^2}{n_e} \exp \left[ \nu' \frac{(n_{\text{bB}} - q)^2}{n_{\text{bB}} n_e} \right] \quad (6a)$$

or in a logarithmic form as

$$\ln \tau_p - \ln \left[ \frac{n_{\text{bB}}(n_{\text{bB}} - q)^2}{n_e} \right] \approx \nu' \frac{(n_{\text{bB}} - q)^2}{n_{\text{bB}} n_e} + \ln \frac{\zeta \nu^2 b^2}{kT} \quad (6b)$$

where  $\zeta$  is the monomeric frictional coefficient of the B segments,  $\nu$  is a constant close to unity, and  $\nu' (= \frac{3}{2}\nu^2)$  is another constant. If  $q = 0$ , i.e., if all segments of the B cilium are trapped in the tube, eq 6 reduces to the original form of the Doi-Kuzuu theory.<sup>10</sup> The detailed derivation of eq 6 from eq 5 is described in our previous paper<sup>3</sup> and is not repeated here.

The two quantities  $q$  and  $n_e$  are estimated respectively as<sup>3</sup>

$$q \approx (r^*/b)^2 \quad r^* = (D/2) - r_s \quad (7a)$$

$$n_e \approx n_e^{\text{bulk}} \rho_e^{\text{bulk}} / \rho_e \quad (7b)$$

where  $D$  is the mean distance between the centers of neighboring micelles,  $r^*$  is the thickness of a spherical shell which is assumed to be filled with the untrapped B cilium segments (see Figure 6c),  $\rho_e$  is the density of the B cilium segment in the tube region, and  $\rho_e^{\text{bulk}}$  is the segment density in bulk homopolybutadiene. The parameters  $r^*$ ,  $\rho_e$  and thus  $q$ ,  $n_e$  are estimated from the structural characteristics of the micelle system, as described in our previous paper.<sup>3</sup> The parameters appearing in eq 6 except for  $\zeta$ ,  $\nu$ , and  $\nu'$  are empirically determined and/or estimated.

Figure 7 shows the relation of  $\ln \tau_p - \ln [n_{bB}(n_{bB} - q)^2/n_e]$  vs.  $(n_{bB} - q)^2/(n_{bB}n_e)$  for the SB/hB blends reduced to 25 °C. Since the assumption that the hB molecules do not contribute to the tube was probably too simple and the estimation of the parameters was also difficult, the data for the blends with  $c$  just above  $c_b^*$  are omitted in this figure. All the results for the SB/hB blends can be satisfactorily represented by a universal curve. This universal relation coincides with that of our modified tube theory, eq 6, for a partially entangled chain with a fixed end. The slope  $\nu'$  ( $=0.7$ ) of the line in this figure is close to the value of 0.66 employed by Doi and Kuzuu<sup>10</sup> for the experimental results on star polymers. From the value of the intersect of the line shown in Figure 7,  $\zeta\nu^2b^2/kT$  is estimated as  $2.8 \times 10^{-5}$  s. Although we could choose a little larger value (i.e., 0.8) of the slope  $\nu'$  and  $\zeta\nu^2b^2/kT$  may be a little smaller than  $2.8 \times 10^{-5}$  s, its magnitude does not change much. Employing the values of  $b = 6.3 \times 10^{-8}$  cm,  $\nu = 0.68$ , and  $kT = 4.11 \times 10^{-14}$  erg, we estimated the monomeric frictional coefficient as  $\zeta = 6 \times 10^{-4}$  (dyn s)/cm (25 °C). This value is about  $10^5$  times larger than the value,  $4 \times 10^{-9}$  (dyn s)/cm (25 °C), reported for linear polybutadiene.<sup>22</sup>

**Discrepancy in the Prefactor.** Since the slow relaxation mechanism for the SB/hB blends is essentially due to the retarded motion of the B blocks, the value of  $\zeta$  must be the same in the blends and bulk hB. However, we found that there exists a discrepancy by a factor of  $10^3$ – $10^5$  between the experimental and theoretical  $\tau_p$ . This result suggests that eq 5 for the region of  $c$  above  $c_b^*$  is slightly modified as

$$\tau_p \cong 10^5 \tau^{(1)} \exp(\Delta U/kT) \quad (5')$$

A plausible explanation for this prefactor may be as follows.<sup>3</sup> When the SB/hB blend undergoes stress relaxation, B cilia escape from the tube confinement, and at the same time, the spatial distribution of the centers of gravity of the micelles becomes the equilibrium one. Namely, not only the relaxation of individual cilia but also the rearrangement of the micelle position should take place. Thus, the longest relaxation time  $\tau_p$  of the blend is expected to be much longer than the reptational time  $\tau^{(1)} \exp(\Delta U/kT)$  of a B cilium defined by eq 5. Even then,  $\tau_p$  seems to be proportional to  $\tau^{(1)} \exp(\Delta U/kT)$  because the latter gives the time scale of the reptation of the individual B cilia, and such a reptation must take place during the micelle rearrangement process.

The micelle rearrangement process may be regarded as a diffusion process of the micelles. The longest relaxation time  $\tau_p$  required for a micelle to diffuse a certain length  $L$  is simply given as

$$\tau_p \cong L^2/D_S \quad (8)$$

where  $D_S$  is the translational diffusion constant of the micelle. By employing the Stokes-Einstein relation,<sup>6</sup>  $D_S$  is given as

$$D_S \cong kT/6\pi R_m \eta_{\text{eff}} \quad (9)$$

where  $R_m$  is the (virtual) radius of the micelle and  $\eta_{\text{eff}}$  the (effective) viscosity of the medium in which the micelle diffuses. Since the micelles in the region of  $c$  above  $c_b^*$  are overlapping each other, the  $R_m$  would assume a value between the actual radius  $R_B + r_S$  of the micelle and the radius  $r_S$  of the S core.

The most important quantity is  $\eta_{\text{eff}}$ . As shown in Figure 4,  $\tau_p$  becomes independent of the molecular weight of hB with increasing  $c$ . This indicates that the viscosity of the medium for the micelle diffusion is determined by the (reptational) motion of the B cilia. Thus,  $\eta_{\text{eff}}$  may be

related to the relaxational time of a B cilium as

$$\eta_{\text{eff}} \cong E \tau^{(1)} \exp(\Delta U/kT) \quad (10)$$

where  $E$  is the (virtual) plateau modulus of the B cilium. From eq 8–10,  $\tau_p$  is written as

$$\tau_p \cong F \tau^{(1)} \exp(\Delta U/kT) \quad (11)$$

where  $F = 6\pi L^2 R_m E/kT$  is the prefactor. This indicates that  $\tau_p$  is proportional to  $\tau^{(1)} \exp(\Delta U/kT)$ . The estimation of  $L$ ,  $R_m$ , and  $E$  includes some arbitrary factors, and it is difficult to determine  $F$  quantitatively. Thus, we estimate  $F$  approximately as follows. The plateau modulus  $E$  would be assigned as  $10^6$ – $10^7$  dyn/cm<sup>2</sup>, which is close to the value for linear homopolybutadiene.<sup>4,5</sup> The energy of thermal motion  $kT$  is about  $4 \times 10^{-14}$  erg (25 °C), and the values of  $L$  and  $R_m$  would not differ much from the micelle dimension (a few hundred angstroms). Thus, the value of  $F$  is approximately estimated as

$$F \cong 6 \times 10^4 - 6 \times 10^5 \quad (\text{if } L \cong R_m \cong 500 \text{ \AA}) \quad (12)$$

This result agrees with eq 5'. Although some uncertainty still remains, the fact that the dependence of  $\tau_p$  on the SB content and the molecular weight of the B block is well described by eq 5 (except the prefactor) seems to justify the above considerations.

The discrepancy of the prefactor in the region of  $c$  below  $c_b^*$  can be explained in a similar manner. Although another difficulty in the  $M_{bB}$  dependence makes the situation more complicated, the tube renewal process must take place during the micelle rearrangement process in this region. The viscosity of the medium for the micelle diffusion in this region would be related to the time  $N_{\text{sub}}^2 \tau_{\text{rep}}/18\pi^2$  (see eq 3) required for the tube renewal process in the same manner as described in eq 10. Thus, the longest relaxation time of the blend in this region seems to be much longer than, but proportional to, the time required for the tube renewal process.

**Acknowledgment.** We are grateful for the support of the Ministry of Education, Science, and Culture (Mombusho) for Grants 347081 and 543026.

**Registry No.** (Styrene)-(butadiene) (copolymer), 9003-55-8; polybutadiene (homopolymer), 9003-17-2.

## References and Notes

- (1) Watanabe, H.; Kotaka, T. *J. Rheol. (N.Y.)* **1983**, *27*, 223.
- (2) Watanabe, H.; Yamao, S.; Kotaka, T. *Nippon Reoroji Gakkaishi* **1982**, *10*, 143.
- (3) Watanabe, H.; Kotaka, T. *Macromolecules* **1983**, *16*, 769.
- (4) Graessley, W. W. *Adv. Polym. Sci.* **1974**, *16*, 48.
- (5) Ferry, D. J. "Viscoelastic Properties of Polymers", 3rd ed.; Wiley: New York, 1980.
- (6) de Gennes, P. G. "Scaling Concepts in Polymer Physics"; Cornell University Press: New York, 1979.
- (7) Doi, M.; Edwards, S. F. *J. Chem. Soc., Faraday Trans. 2* **1978**, *74*, 1789, 1802, 1818; *Ibid.* **1979**, *75*, 38.
- (8) Doi, M. *J. Polym. Sci., Polym. Phys. Ed.* **1980**, *18*, 1005, 1981.
- (9) Evans, K. E.; Edwards, S. F. *J. Chem. Soc., Faraday Trans. 2* **1981**, *77*, 1891, 1913, 1929.
- (10) Doi, M.; Kuzuu, N. *J. Polym. Sci., Polym. Lett. Ed.* **1980**, *18*, 775.
- (11) Watanabe, H.; Kotaka, T. *Polym. J.* **1982**, *14*, 739.
- (12) Inoue, T.; Soen, T.; Hashimoto, T.; Kawai, H. *Macromolecules* **1970**, *3*, 87.
- (13) Kotaka, T.; Miki, T.; Arai, K. *J. Macromol. Sci., Phys.* **1980**, *B17*, 303.
- (14) Ramos, A. R.; Cohen, R. E. *Polym. Eng. Sci.* **1977**, *17*, 639. Cohen, R. E.; Ramos, A. R. *Macromolecules* **1979**, *12*, 131. Cohen, R. E.; Wilfong, D. E. *Macromolecules* **1982**, *15*, 370.
- (15) Hashimoto, T.; Shibayama, M.; Kawai, H.; Watanabe, H.; Kotaka, T. *Macromolecules* **1983**, *16*, 361.
- (16) Markovitz, H. *J. Appl. Phys.* **1952**, *23*, 1070.
- (17) Tschoegl, N. W. *Rheol. Acta* **1971**, *10*, 582.
- (18) Doi, M. *Chem. Phys. Lett.* **1974**, *26*, 269.



- (19) de Gennes, P. G. *Macromolecules* 1976, 9, 587, 594.  
 (20) Klein, J. *Macromolecules* 1978, 11, 852.  
 (21) Graessley, W. W. *Adv. Polym. Sci.* 1982, 47, 97. (In this paper, the words "constraint release" are used instead of "tube renewal".)  
 (22) Estimated from the experimental data for the zero-shear viscosity and steady-state recoverable compliance reported by Graessley and co-workers (ref 23).  
 (23) Raju, V. R.; Menezes, E. V.; Marin, G.; Graessley, W. W.; Fetters, L. J. *Macromolecules* 1981, 14, 1668.

## Viscoelastic Relaxations in Oxidized Poly(hexamethylene sulfide)

José M. Pereña, Carlos Marco, Antonio Bello, and José G. Fatou\*

Unidad de Física y Fisicoquímica de Polímeros, Instituto de Plásticos y Caucho, CSIC, Madrid-6, Spain. Received February 24, 1983

**ABSTRACT:** The dynamic mechanical behavior of several oxidized poly(hexamethylene sulfide) samples has been studied. Two relaxations that have been found and considered were a low-temperature  $\gamma$  relaxation of polymethylenic units and a higher temperature  $\beta$  transition. The presence and variations of these relaxations have been discussed in relation to the composition of the different samples.

### Introduction

Poly(thioethers) with the general structure  $[-(\text{CH}_2)_m-\text{S}-]_n$  can be obtained by different polymerization methods. For example, poly(hexamethylene sulfide) can be prepared by polymerizing hexamethylenedithiol and bialllyl, using ammonium persulfate and sodium metabisulfite to initiate the reaction. Moreover, the oxidation of poly(alkyl sulfides) is a method for obtaining poly(alkyl sulfones) with the general formula  $[-(\text{CH}_2)_m-\text{SO}_2-]_n$ . Poly(alkyl sulfonates), in the intermediate stage of the reaction, are usually oxidized to poly(sulfones), depending on the experimental conditions, and only a few reactions allow selective oxidation of sulfides to sulfoxides.

Different degrees of sulfonation and sulfoxidation can thus be obtained by modifying the experimental conditions. For this reason many of the data on the thermal transitions of these polymers involve some dispersion and confusion due to variations in molecular weight and molecular structure resulting from the method of synthesis.

In a previous paper<sup>1</sup> we reported the oxidation of poly(hexamethylene sulfide) crystallized in very dilute solutions in order to investigate the oxidative attack and the properties of the polysulfone products. Changes in the enthalpy and temperature of melting have been found and correlated with different stages of the oxidation. These stages correspond to different compositions in sulfide, sulfoxide, and sulfone groups, modifying not only the transition temperatures but especially the crystalline structure.

Since the study of dynamic relaxations may lead to a better knowledge of the nature of the fold surface of crystallites because the oxidative attack takes place preferentially in the noncrystalline regions,<sup>2</sup> the aim of this work is to study how the dynamic mechanical relaxations of several oxidized poly(hexamethylene sulfide) samples are changed by the variation in the composition of the resulting polymers.

### Experimental Section

**Materials.** The preparation of poly(hexamethylene sulfide) (PS1) was carried out by polymerization of hexamethylenedithiol and bialllyl, using ammonium persulfate and sodium metabisulfite to initiate the reaction, according to the method described by Marvel and Aldrich.<sup>3</sup> The crude polymer product was dissolved in chloroform, and methanol was added as a precipitant. The precipitate was recovered by filtration and dried in a vacuum desiccator. The first precipitated polymer was fractionated with benzene/methanol. The number-average molecular weight was

Table I  
Composition of Oxidized Poly(hexamethylene sulfide) (PS) with Different Amounts of Sulfoxide (PSO) and Sulfone (PSDO) Groups

sample	wt fraction/%		
	PS	PSO	PSDO
PS1 <sup>a</sup>	100	0	0
PS2 <sup>a</sup>	75	25	0
PS3 <sup>a</sup>	60	40	ca. 0
PS4 <sup>a</sup>	35	30	35
PS5 <sup>a</sup>	40	35	25
PS6 <sup>b</sup>	ca. 0	ca. 100	ca. 0

<sup>a</sup> Semicrystalline sample. <sup>b</sup> Amorphous sample.

measured in a Hitachi Perkin-Elmer vapor pressure osmometer at 25 °C in chloroform solution. The resulting  $\bar{M}_n$  was 9000.

Almost pure poly(hexamethylene sulfoxide) (PS6) was obtained from a PS1 sample ( $\bar{M}_n = 10800$ ) by oxidation in solution. A 0.346-g sample of PS1 was dissolved in 50 mL of chloroform. To this solution, 0.13 mol of 30% hydrogen peroxide was added with vigorous stirring at 25 °C. After 2 h, the solution was evaporated under vacuum, yielding a heterogeneous film, which was dissolved in chloroform and was precipitated by addition of methanol. The white solid was separated by filtration and then was repeatedly washed with ethanol and vacuum-dried. Quantitative elemental analysis of C, H, and S was carried out in a Perkin-Elmer 240 analyzer: C, 54.84; H, 9.20; S, 23.95 (calcd: C, 54.55; H, 9.09; S, 24.24). The infrared spectrum showed the sulfoxide band at 1030  $\text{cm}^{-1}$ , but not the band at 1130  $\text{cm}^{-1}$  for the sulfone group. X-ray diffraction showed no crystallinity. Both the PS1 and PS6 films were cast from chloroform solution.

PS2 and PS3 films were made from preformed samples of PS1, immersed in 50 mL of water, and oxidized at 25 °C with  $7 \times 10^{-4}$  and  $15 \times 10^{-3}$  M solutions, respectively, of aqueous hydrogen peroxide (30%) under continuous stirring for 24 h. Oxidized films were thoroughly washed with ethanol and dried in a vacuum desiccator for 24 h. PS4 and PS5 films were obtained as described above, but with solutions of aqueous hydrogen peroxide (30%) dissolved in aqueous  $2.5 \times 10^{-2}$  M trifluoroacetic acid.

The compositions of all the samples are listed in Table I.

**X-ray Diffraction.** X-ray diffraction measurements were made with a Philips X-ray diffractometer. The diagrams were recorded in the  $2\theta$  range between 4 and 35°, with nickel-filtered  $\text{Cu K}\alpha$  radiation.

**Thermal Properties.** The thermal properties were studied in a DuPont DSC-900 calorimeter. The weights of the samples ranged between 3 and 7 mg and the heating rate was 10 °C/min.  $T_g$  was taken as the intersection of the base line with the extrapolated sloping portion of the curve produced when a base line shift occurred during the transition.